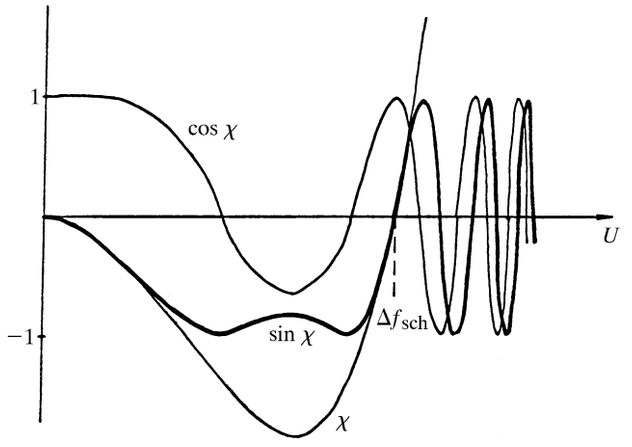

Fig. 2.5.5.1. The χ function and two components of the Scherzer phase function $\sin \chi(U)$ and $\cos \chi(U)$.

$q(\mathbf{x}) = \exp[-i\sigma\varphi(\mathbf{x})]$ (2.5.2.42), and for weak phase objects the approximation $[\sigma\varphi \ll 1]$

$$q(\mathbf{x}) = 1 - i\sigma\varphi(\mathbf{x}) \tag{2.5.5.5}$$

is valid.

In the back focal plane of the objective lens the wave has the form

$$Q(uv) \cdot T(U) \tag{2.5.5.6}$$

$$T = A(U)\exp(i\chi U) \tag{2.5.5.7a}$$

$$\chi(U) = \pi\Delta f\lambda U^2 + \frac{\pi}{2}C_s\lambda^3 U^4, \tag{2.5.5.7b}$$

where $U = (u^2 + v^2)^{1/2}$; $\exp[i\chi(U)]$ is the Scherzer phase function (Scherzer, 1949) of an objective lens (Fig. 2.5.5.1), $A(U)$ is the aperture function, C_s the spherical aberration coefficient, and Δf the defocus value [(2.5.2.32)–(2.5.2.35)].

The bright-field image intensity (in object coordinates) is

$$I(xy) = |\psi_1(xy) * t(xy)|^2, \tag{2.5.5.8}$$

where $t = \mathscr{F}^{-1}[T]$. The phase function (2.5.5.7) depends on defocus, and for a weak phase object (Cowley, 1981)

$$I(xy) = 1 + 2\sigma\varphi(xy) * s(xy), \tag{2.5.5.9}$$

where $s = \mathscr{F}^{-1}[A(U)\sin\chi]$, which includes only an imaginary part of function (2.5.5.6). While selecting defocus in such a way that under the Scherzer defocus conditions [(2.5.2.44), (2.5.2.45)] $|\sin\chi| \simeq 1$, one could obtain

$$I(xy) = 1 + 2\sigma\varphi(xy) * a(xy). \tag{2.5.5.10}$$

In this very simple case the image reflects directly the structure of the object – the two-dimensional distribution of the projection of the potential convoluted with the spread function $a = \mathscr{F}^{-1}A$. In this case, no image restoration is necessary. Contrast reversal may be achieved by a change of defocus.

At high resolution, this method enables one to obtain an image of projections of the atomic structure of crystals and defects in the atomic arrangement – vacancies, replacements by foreign atoms, amorphous structures and so on; at resolution worse than atomic one obtains images of dislocations as continuous lines, inserted phases, inclusions *etc.* (Cowley, 1981). It is also possible to obtain images of thin biological crystals, individual molecules, biological macromolecules and their associations.

Image restoration. In the case just considered (2.5.5.10), the projection of potential $\varphi(xy)$, convoluted with the spread function, can be directly observed. In the general case (2.5.5.9), when the aperture becomes larger, the contribution to image formation is made by large values of spatial frequencies U, in which the function $\sin\chi$ oscillates, changing its sign. Naturally, this distorts the image just in the region of appropriate high resolution. However, if one knows the form of the function $\sin\chi$ (2.5.5.7), the true function $\varphi(xy)$ can be restored.

This could be carried out experimentally if one were to place in the back focal plane of an objective lens a zone plate transmitting only one-sign regions of $\sin\chi$ (Hoppe, 1971). In this case, the information on $\varphi(xy)$ is partly lost, but not distorted. To perform such a filtration in an electron microscope is a rather complicated task.

Another method is used (Erickson & Klug, 1971). It consists of a Fourier transformation $\mathscr{F}^{-1}$ of the measured intensity distribution TQ (2.5.5.6) and division of this transform, according to (2.5.5.7*a*,*b*), by the phase function $\sin\chi$. This gives

$$\frac{TQ}{\sin\chi} = Q(uv)A(U). \tag{2.5.5.11a}$$

Then, the new Fourier transformation $\mathscr{F}QA$ yields (in the weak-phase-object approximation) the true distribution

$$\varphi(xy) * a(xy). \tag{2.5.5.11b}$$

The function $\sin\chi$ depending on defocus Δf should be known to perform this procedure. The transfer function can also be found from an electron micrograph (Thon, 1966). It manifests itself in a circular image intensity modulation of an amorphous substrate or, if the specimen is crystalline, in the 'noise' component of the image. The analogue method (optical Fourier transformation for obtaining the image $\sin\chi$) can be used (optical diffraction, see below); digitization and Fourier transformation can also be applied (Hoppe *et al.*, 1973).

The thin crystalline specimen implies that in the back focal objective lens plane the discrete kinematic amplitudes Φ_{hk} are arranged and, by the above method, they are corrected and released from phase distortions introduced by the function $\sin\chi$ (see below) (Unwin & Henderson, 1975).

For the three-dimensional reconstruction (see Section 2.5.6) it is necessary to have the projections of potential of the specimen tilted at different angles α to the beam direction (normal beam incidence corresponds to $\alpha = 0$). In this case, the defocus Δf changes linearly with increase of the distance l of specimen points from the rotation axis $\Delta f_\alpha = \Delta f_0(1 + l\sin\alpha)$. Following the above procedure for passing on to reciprocal space and correction of $\sin\chi$, one can find $\varphi_\alpha(xy)$ (Henderson & Unwin, 1975).

2.5.5.3. An account of absorption

Elastic interaction of an incident wave with a weak phase object is defined on its exit surface by the distribution of potential projection $\varphi(xy)$; however, in the general case, the electron scattering amplitude is a complex one (Glauber & Schomaker, 1953). In such a way, the image itself has the phase and amplitude contrast. This may be taken into account if one considers not only the potential projection $\varphi(xy)$, but also the 'imaginary potential'

$\mu(xy)$ which describes phenomenologically the absorption in thin specimens. Then, instead of (2.5.5.5), the wave on the exit surface of a specimen can be written as

$$q(xy) = 1 - i\sigma\varphi(xy) - \mu(xy) \tag{2.5.5.12}$$

and in the back focal plane if $\Phi = \mathscr{F}\varphi$ and $M = \mathscr{F}\mu$

$$Q(uv) = \delta(uv) - i\sigma\Phi(uv) - M(uv). \tag{2.5.5.13}$$

Usually, μ is small, but it can, nevertheless, make a certain contribution to an image. In a sufficiently good linear approximation, it may be assumed that the real part $\cos\chi$ of the phase function (2.5.5.7*a*) affects $M(uv)$, while $\Phi(xy)$, as we know, is under the action of the imaginary part $\sin\chi$.

Thus, instead of (2.5.5.6), one can write

$$Q(\exp i\chi) = \delta(\mathbf{u}) - i\sigma\Phi(\mathbf{u})\sin\chi - M(\mathbf{u})\cos\chi, \tag{2.5.5.14}$$

and as the result, instead of (2.5.5.10),

$$\begin{aligned} I(xy) = 1 &+ 2\sigma\varphi(xy) * \mathscr{F}^{-1}(\sin\chi) * a(U) \\ &- 2\mu(xy) * \mathscr{F}^{-1}(\cos\chi) * a(U). \end{aligned} \tag{2.5.5.15}$$

The functions $\varphi(xy)$ and $\mu(xy)$ can be separated by object imaging using the through-focus series method. In this case, using the Fourier transformation, one passes from the intensity distribution (2.5.5.15) in real space to reciprocal space. Now, at two different defocus values Δf_1 and Δf_2 [(2.5.5.6), (2.5.5.7*a*,*b*)] the values $\Phi(\mathbf{u})$ and $M(\mathbf{u})$ can be found from the two linear equations (2.5.5.14). Using the inverse Fourier transformation, one can pass on again to real space which gives $\varphi(\mathbf{x})$ and $\mu(\mathbf{x})$ (Schiske, 1968). In practice, it is possible to use several through-focus series and to solve a set of equations by the least-squares method.

Another method for processing takes into account the simultaneous presence of noise $N(\mathbf{x})$ and transfer function zeros (Kirkland *et al.*, 1980). In this method the space frequencies corresponding to small values of the transfer function modulus are suppressed, while the regions where such a modulus is large are found to be reinforced.

2.5.5.4. Thick crystals

When the specimen thickness exceeds a certain critical value (~50–100 Å), the kinematic approximation does not hold true and the scattering is dynamic. This means that on the exit surface of a specimen the wave is not defined as yet by the projection of potential $\varphi(xy) = \int\varphi(\mathbf{r})\,\mathrm{d}z$ (2.5.5.3), but one has to take into account the interaction of the incident wave ψ_0 and of all the secondary waves arising in the whole volume of a specimen.

The dynamic scattering calculation can be made by various methods. One is the multislice (or phase-grating) method based on a recurrent application of formulae (2.5.5.3) for n thin layers Δz_i thick, and successive construction of the transmission functions q_i (2.5.5.4), phase functions $Q_i = \mathscr{F}q_i$, and propagation function $p_k = [k/2\pi i\Delta z]\exp[ik(x^2 + y^2)/2\Delta z]$ (Cowley & Moodie, 1957).

Another method – the scattering matrix method – is based on the solution of equations of the dynamic theory (Chapter 5.2). The emerging wave on the exit surface of a crystal is then found to diffract and experience the transfer function action [(2.5.5.6), (2.5.5.7*a*,*b*)].

The dynamic scattering in crystals may be interpreted using Bloch waves:

$$\Psi^j(\mathbf{r}) = \sum_H C_H^j \exp(-2\pi i\mathbf{k}_H^j \cdot \mathbf{r}). \tag{2.5.5.16}$$

It turns out that only a few (bound and valence Bloch waves) have strong excitation amplitudes. Depending on the thickness of a crystal, only one of these waves or their linear combinations (Kambe, 1982) emerges on the exit surface. An electron-microscopic image can be interpreted, at certain thicknesses, as an image of one of these waves [with a correction for the transfer function action (2.5.5.6), (2.5.5.7*a*,*b*)]; in this case, the identical images repeat with increasing thickness, while, at a certain thickness, the contrast reversal can be observed. Only the first Bloch wave which arises at small thickness, and also repeats with increasing thickness, corresponds to the projection of potential $\varphi(xy)$, *i.e.* the atom projection distribution in a thin crystal layer.

An image of other Bloch waves is defined by the function $\varphi(\mathbf{r})$, but their maxima or minima do not coincide, in the general case, with the atomic positions and cannot be interpreted as the projection of potential. It is difficult to reconstruct $\varphi(xy)$ from these images, especially when the crystal is not ideal and contains imperfections. In these cases one resorts to computer modelling of images at different thicknesses and defocus values, and to comparison with an experimentally observed pattern.

The imaging can be performed directly in an electron microscope not by a photo plate, but using fast-response detectors with digitized intensity output online. The computer contains the necessary algorithms for Fourier transformation, image calculation, transfer function computing, averaging, and correction for the observed and calculated data. This makes possible the interpretation of the pattern observed directly in experiment (Herrmann *et al.*, 1980).

2.5.5.5. Image enhancement

The real electron-microscope image is subdivided into two components:

$$J(xy) = I(xy) + N(xy). \tag{2.5.5.17}$$

The main of these, $I(xy)$, is a two-dimensional image of the 'ideal' object obtained in an electron microscope with instrumental functions inherent to it. However, in the process of object imaging and transfer of this information to the detector there are various sources of noise. In an electron microscope, these arise owing to emission-current and accelerating-voltage fluctuations, lens-supplying current (temporal fluctuations), or mechanical instabilities in a device, specimen or detector (spatial shifts). The two-dimensional detector (*e.g.* a photographic plate) has structural inhomogeneities affecting a response to the signal. In addition, the specimen is also unstable; during preparation or imaging it may change owing to chemical or some other transformations in its structure, thermal effects and so on. Biological specimens scatter electrons very weakly and their natural state is moist, while in the electron-microscope column they are under vacuum conditions. The methods of staining (negative or positive), *e.g.* of introducing into specimens substances containing heavy atoms, as well as the freeze-etching method, somewhat distort the structure of a specimen. Another source of structure perturbation is radiation damage, which can be eliminated at small radiation doses or by using the cryogenic technique. The structure of stained specimens is affected by stain graininess. We assume that all the deviations $\Delta I_k(xy)$ of a specimen image from the 'ideal' image $I_k(xy)$ are included in the noise term $N_k(xy)$. The substrate may also be inhomogeneous. All kinds of perturbations cannot be separated and they appear on an electron microscope image as the full noise content $N(xy)$.